

Metabolic biochemical models of N₂ fixation for sulfide oxidizers, methanogens, and methanotrophs

Meng Gao,¹ Megan E. Berberich,² Reid Brown,³ David M. Costello,⁴ James B. Cotner,^{5,6} Julian Damashek,⁷ Leila Richards Kittu,⁸ Ada Pastor,⁹ Robinson W. Fulweiler,¹⁰ J. Thad Scott,¹¹ Amy M. Marcarelli,² Keisuke Inomura¹

AUTHOR AFFILIATIONS See affiliation list on p. 14.

ABSTRACT Dinitrogen (N₂) fixation provides bioavailable nitrogen to the biosphere. However, in some habitats (e.g., sediments), the metabolic pathways of organisms carrying out N₂ fixation are unclear. We present metabolic models representing various chemotrophic N₂ fixers, which simulate potential pathways of electron transport and energy flow, resulting in predictions of whole-cell stoichiometries. By balancing mass, electrons, and energy for metabolic half-reactions, we quantify the electron usage for nine N₂ fixers. Our results demonstrate that all modeled organisms fix sufficient N₂ for growth. Aerobic organisms allocate more electrons to N₂ fixation and growth, yielding more biomass and fixing more N₂, while methanogens using acetate and organisms using sulfate allocate fewer electrons. This work can be applied to investigate the depth distribution of N₂ fixers based on nutrient availability, complementing field measurements of biogeochemical processes and microbial communities.

IMPORTANCE N₂ fixation is an important process in the global N cycle. Researchers have developed models for heterotrophic and photoautotrophic N₂ fixers, but there is a lack of modeling studies on chemoautotrophic N₂ fixers. Here, we built nine biochemical models for different chemoautotrophic N₂ fixers by combining different types of half-chemical reactions. We include three sulfide oxidizers using different electron acceptors (O₂, NO₃⁻, and Fe³⁺), contributing to the sulfur, nitrogen, and iron cycles in the sediment. We have two methanogens using different substrates (H₂ and acetate) and four methanotrophs using different electron acceptors (O₂, NO₃⁻, Fe³⁺, and SO₄²⁻). By modeling these methane producers and users in the sediment and their N₂-fixing metabolic pathways, our work can provide insight for future carbon cycle studies. This study outlines various metabolic pathways that can facilitate N₂ fixation, with implications for where in the environment they might occur.

KEYWORDS N₂ fixation, biochemical model, sulfide oxidizers, methanogens, methanotrophs, sediment, electron allocation, energy, CFM-CNF

Biological dinitrogen (N₂) fixation, one of the key pathways in the global nitrogen (N) cycle, provides bioavailable N to the global biosphere (1–5). N₂ fixation is widespread across the Earth (6) and is found in various environments, including oligotrophic oceans (7), deep seas (8), nutrient-rich coastal waters (9), and the cold Arctic (5, 10, 11). However, in some ecosystems with high organismal and habitat diversity (e.g., wetlands, seagrass meadows, estuaries), estimating N₂ fixation rates and their drivers remains challenging (12, 13). In order to explore N₂ fixation mechanisms, it is important to consider the N₂ fixation reaction itself (equation 1), which shows that N₂ fixation requires electrons and a large amount of energy (16 ATP per N₂). As a result, sources of electrons and energy are important while considering this process. Redox and electron acceptor availability tend to shape the depth distribution of N₂ fixers in

Editor Ashkaan K. Fahimipour, Florida Atlantic University, Boca Raton, Florida, USA

Address correspondence to Meng Gao, meng_gao@uri.edu.

The authors declare no conflict of interest.

See the funding table on p. 15.

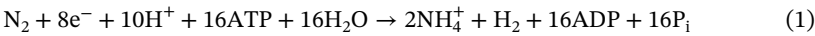
Received 28 May 2025

Accepted 1 July 2025

Published 8 September 2025

Copyright © 2025 Gao et al. This is an open-access article distributed under the terms of the [Creative Commons Attribution 4.0 International license](https://creativecommons.org/licenses/by/4.0/).

aquatic sediments, determining where N₂ fixation occurs. Investigating these patterns is essential for understanding how N₂ fixation contributes to global nitrogen and carbon cycling.



Modeling studies of diazotrophic metabolism have primarily focused on N₂ fixation by photoautotrophic cyanobacteria (14–16) and, to a lesser extent, heterotrophic bacteria (12, 17, 18). However, other “chemotrophic” energy-generating pathways can be coupled to N₂ fixation, including methane oxidation, methanogenesis, and sulfur oxidation. Little is known about N₂ fixation by chemoautotrophs, despite their crucial role in Earth’s biogeochemical history and continued prevalence in marine and freshwater systems, nor have models of these organisms been developed. Quantitative models can help predict potentially viable chemoautotrophic metabolic pathways to provide electrons and energy for N₂ fixation (17, 19–22). Here, we constructed nine biochemical models for nine chemoautotrophs with different resource utilizations (Table 1). We named them cell flux models of chemotrophic nitrogen fixers (CFM-CNF).

Electrons for N₂ fixation can be provided by some carbon (C) oxidation reactions (4, 23–25). For example, evidence shows that in methanotrophs, which are organisms that metabolize methane as their chemical energy source, methane oxidation can be coupled to N₂ fixation (26), with electrons transferred both to N₂ and to electron acceptors for energy production. For example, O₂ is a favorable electron acceptor in oxic environments, while in anoxic environments, NO₃[−] (27), Fe³⁺ (28), and the less favorable acceptor SO₄^{2−} (29) are all reported as electron acceptors in methanotrophs (30, 31). These various electron acceptors distinguish different types of methanotrophs: O₂ reducers, NO₃[−] reducers, Fe reducers, and SO₄^{2−} reducers. We included these four different types of methanotrophs in this modeling study to represent the variation of these electron acceptors in different habitats.

In the global carbon cycle, methanogens, which are organisms that can produce methane, also play an important role. The methane production processes are electron-accepting reactions that can reduce CO₂ to methane and release energy. Hydrogen (H₂) and acetate are important substrates for methanogens (32, 33). Some methanogens have also been reported as N₂ fixers, which broadens the organisms capable of N₂ fixation into the Archaea (34). However, more studies are needed to explore the coupling mechanism between methanogenesis and N₂ fixation as part of a suite of possible metabolic pathways that could support N₂ fixation. In this study, we include methanogen (acetate and H₂ oxidizers) models to investigate the mechanism in detail.

Previous studies have also reported that sulfur oxidation, an electron-donating reaction, can be coupled with N₂ fixation in sediments (35, 36) as an electron source. Sulfide-oxidizing microorganisms are commonly reported in sulfidic water columns (37), marine and lake sediments (38, 39), microbial mats (40), and hydrothermal vents (41).

TABLE 1 Models and the applied half reactions^a

Model	Rd (donation)	Ra (acceptance)
Sulfide oxidizer (O ₂)	2	6
Sulfide oxidizer (NO ₃ [−])	2	7
Sulfide oxidizer (Fe ³⁺)	2	8
Methanogen (acetate)	3	9
Methanogen (H ₂)	4	9
Methanotroph (O ₂)	5	6
Methanotroph (NO ₃ [−])	5	7
Methanotroph (Fe ³⁺)	5	8
Methanotroph (SO ₄ ^{2−})	5	10

^aNote: equations 2 to 10 are half reactions listed in Table 2 (Rd) and (Table 3) (Ra). For all of the models, Rn (N₂ fixation) is equation 1 listed in the introduction, and Rc (biosynthesis) is equation 11.

TABLE 2 A list of half reactions for electron donors (Rd)

Chemical equation	Equation number
$\frac{1}{8} \text{H}_2\text{S} + \frac{1}{2} \text{H}_2\text{O} = \frac{1}{8} \text{SO}_4^{2-} + \frac{5}{4} \text{H}^+ + \text{e}^-$	2
$\frac{1}{8} \text{CH}_3\text{COO}^- + \frac{3}{8} \text{H}_2\text{O} = \frac{1}{8} \text{CO}_2 + \frac{1}{8} \text{HCO}_3^- + \text{e}^- + \text{H}^+$	3
$\frac{1}{2} \text{H}_2 = \text{H}^+ + \text{e}^-$	4
$\frac{1}{4} \text{H}_2\text{O} + \frac{1}{8} \text{CH}_4 = \frac{1}{8} \text{CO}_2 + \text{H}^+ + \text{e}^-$	5

These sulfide oxidizers can use O₂ (39), NO₃[−] (42, 43), and Fe³⁺ reduction (44) to provide energy, and all of these reactions have been reported to have a coupling effect with N₂ fixation (7, 45, 46).

For all of these organisms above (including methanotrophs [O₂ reducers, NO₃[−] reducers, Fe³⁺ reducers, and SO₄^{2−} reducers], methanogens [H₂ oxidizers, and acetate oxidizers], and sulfide oxidizers [O₂ reducers, NO₃[−] reducers, Fe³⁺ reducers]; Table 1), more studies are needed to investigate the potential chemical pathways or use energetic data to understand how N₂ fixation affects their growth or ecology. Each of the nine biochemical models built in this study includes four different types of reactions (Fig. 1a): an electron donation reaction (Rd) to donate the electrons to the reductive half-reactions including synthesis and energy providers; a N₂ fixation (Rn) half-reaction and a biosynthesis (Rc) half-reaction to fix N₂ and grow, and an electron acceptance reaction (Ra) to provide enough energy for the N₂ fixation and biosynthesis. The constructed models integrate both the sources and usage of electrons and energy and consider N₂ fixation and growth, which are two essential processes in the cells of N₂ fixers. This model framework was adapted from Rittmann and McCarty (47) and follows the fundamental laws of mass, electron, and energy conservation. Based on these energy relationships, we calculated electron allocation, biomass yield, and N₂ fixation yield (Fig. 1b) and compared these results among the nine N₂ fixers. Our models address the following questions. (i) What key biochemical reactions are coupled with N₂ fixation in different chemoautotrophs? (ii) How are electrons allocated to different biochemical reactions in these organisms? (iii) How do electron acceptor efficiencies influence N₂ fixation and growth?

RESULTS AND DISCUSSION

Our study includes nine different models: sulfide oxidizers (O₂ reducers, NO₃[−] reducers, Fe³⁺ reducers), methanogens (H₂ oxidizers and acetate oxidizers), and methanotrophs (O₂ reducers, NO₃[−] reducers, Fe³⁺ reducers, and SO₄^{2−} reducers), which have all been listed in Table 1. The first step of our simulation was to determine the appropriate half-reactions (Ra, Rd, Rn, Rc) for each model.

TABLE 3 A list of half reactions for electron acceptors (Ra)

Chemical equation	Equation number
$\frac{1}{4} \text{O}_2 + \text{H}^+ + \text{e}^- = \frac{1}{2} \text{H}_2\text{O}$	6
$\frac{1}{8} \text{NO}_3^- + \frac{5}{4} \text{H}^+ + \text{e}^- = \frac{1}{8} \text{NH}_4^+ + \frac{3}{8} \text{H}_2\text{O}$	7
$\text{Fe}^{3+} + \text{e}^- = \text{Fe}^{2+}$	8
$\frac{1}{8} \text{CO}_2 + \text{H}^+ + \text{e}^- = \frac{1}{4} \text{H}_2\text{O} + \frac{1}{8} \text{CH}_4$	9
$\frac{1}{8} \text{SO}_4^{2-} + \frac{5}{4} \text{H}^+ + \text{e}^- = \frac{1}{8} \text{H}_2\text{S} + \frac{1}{2} \text{H}_2\text{O}$	10

Overview of the half-chemical reactions

Here, we describe how we built the CFM-CNF by using four different half-chemical reactions (Table 1; Fig. S1). For sulfide oxidizers, they oxidize the sulfide to provide electrons and can use O_2 , NO_3^- , and Fe^{3+} as electron acceptors. So, we considered sulfide oxidation (equation 2) as Rd and included O_2 (equation 6), NO_3^- (equation 7), and Fe^{3+} reduction (equation 8) (39, 42, 43) as Ra for different types of sulfide oxidizers (Table 1). For methanogens, their key characteristic is to produce methane, so we consider the methane-producing half-reaction (equation 9) as the electron acceptance (Ra). There are different types of methanogens using different substrates to provide energy and electrons, including acetate (equation 3) and H_2 reduction (equation 4) (48), so we use these two as the two different Rd for two methanogens. Methanotrophs oxidize methane to provide electrons and energy, so we used methane oxidation (equation 5) as the Rd for the methanotroph models. To provide enough energy, they can reduce O_2 (equation 6), NO_3^- (equation 7), Fe^{3+} (equation 8), and SO_4^{2-} (equation 10) (27–29). We used these half reactions as Ra for different methanotrophs. The half-reactions to represent Rn and Rc are listed as equations 1 and 11, which show the general N_2 fixation and growth processes (47).

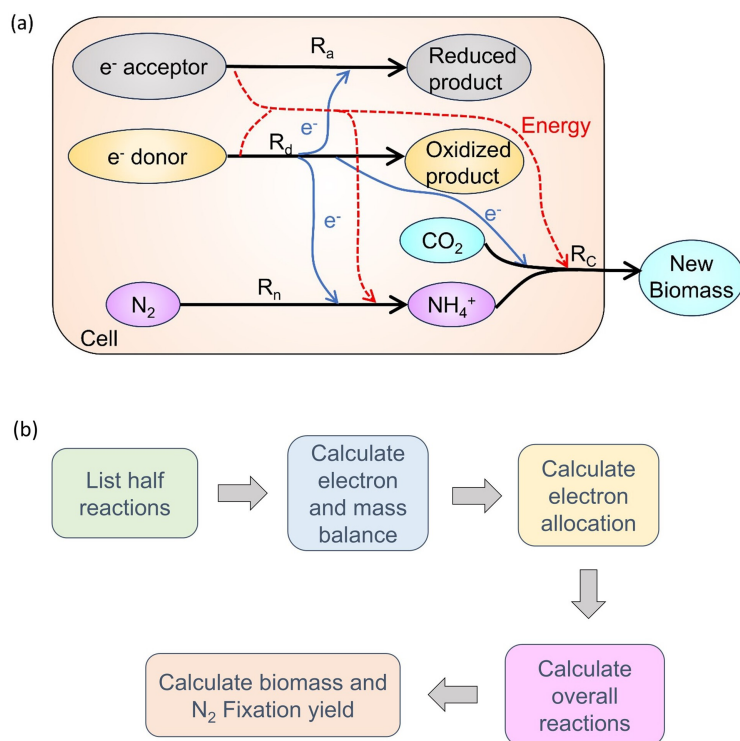
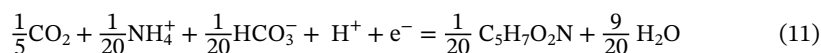


FIG 1 Model and simulation. (a) CFM-CNF schematic. Black arrows mean four main reaction types: R_a (electron acceptance), R_d (electron donation), R_n (N_2 fixation), and R_c (biosynthesis via C fixation). Blue arrows mean electron flow from R_d to others. Red dash arrows mean energy flow. (b) Workflow to do the simulation. For each of the models, we listed the potential chemical reactions included, balanced the electrons and mass, and calculated the electron allocation. We added all the half reactions and calculated the overall reactions. Based on overall reactions, we calculate the biomass and N_2 fixation yield and do the comparison.

Electron allocation

These half-reactions are essential to understanding how electrons are allocated to different cellular processes (e.g., N_2 fixation) across these nine organisms. Our models simulate the electron allocations, which represent the number of electrons allocated to each half-reaction (Ra, Rc, and Rn) if there is one electron released from Rd. When we compare the allocation to Rc and Rn among different models (Fig. 2; Table S2), methanotrophs (O_2) have the highest proportion of electrons dedicated to biosynthesis (0.456) and N_2 fixation (0.091) (Fig. 2; Table S2). Previous evidence showed that methane oxidation under aerobic conditions can enhance N_2 fixation (26), which is consistent with our model results. Methanotrophs (except for when SO_4^{2-} is the electron acceptor) use more electrons in Rc and Rn than sulfide oxidizers, yet the opposite is true for Ra (Fig. 2). Evidence for methanotrophic N_2 fixers has been reported in previous cultural and genetic studies: with the sequencing of *nifH* fragments, researchers found that both types I and II methanotrophs could fix N_2 (49). In studies of wetlands (26) and root tissues of paddy rice (50), N_2 fixation activity was also observed. Our results indicate the theoretical electron acceptance pathways for these methanotrophs and suggest that aerobic pathways could be those with the highest electron efficiency.

Methanogens (acetate) and methanotrophs (SO_4^{2-}) use more electrons in Ra and less in Rc and Rn. Although the electrons used in Rc and Rn are low, these values still exist, meaning these processes can still happen in methanogens (acetate) and methanotrophs

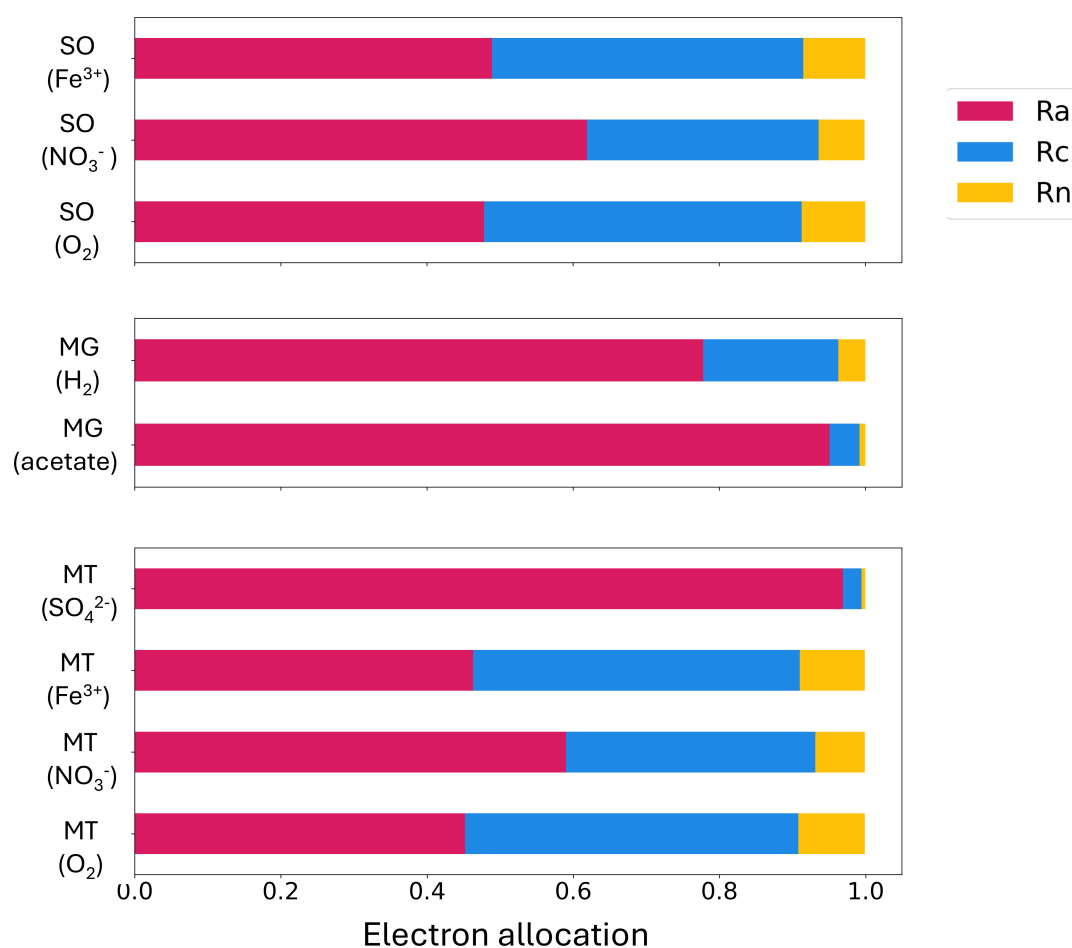


FIG 2 Electron allocation for different organisms. SO: sulfide oxidizers (top panel). MG: methanogens (middle panel). MT: methanotroph (bottom panel). The length of the bars represents electron usage in different reactions. Pink bars are electrons used for Ra (electron acceptance), blue bars are electrons used in Rc (biosynthesis via C fixation), and yellow bars are electrons used for Rn (N_2 fixation). The parentheses mean different electron acceptors or donors for different models.

(SO_4^{2-}). This is consistent with the previous studies: for methanotrophs using SO_4^{2-} , studies found that they can live with only N_2 sources (49). For methanogens, a previous wetland study suggested that organic matter could be the electron donors for methanogens, and they can fix N_2 (26). Our results suggest that although methane and SO_4^{2-} used in these two organisms may not provide large amounts of energy to support biosynthesis and N_2 fixation, their electron donation pathways, including acetate oxidation and methane oxidation, could provide enough energy for their survival and N_2 fixation. These results indicate that in some sedimentary environments with organic C, methane, and SO_4^{2-} , N_2 fixers can exist and may be supported by the half-reactions such as acetate oxidation, methane oxidation, methanogenesis, and SO_4^{2-} reduction. Our result in electron allocation indicates how electrons are distributed among chemical reactions, influencing reaction rates and ultimately affecting biomass and N_2 fixation yields.

Overall reactions and yield: biomass and nitrogen yield per electron

Based on the half-reactions and potential electron and energy relationships listed above, we calculated the coefficient of each half-reaction and added all reactions together to obtain nine overall reaction equations (see Table S1), representing the nine different model metabolic organisms. We assume there is one transported electron for each reaction to normalize the equation. Based on these overall reactions, we can compare biomass and N_2 fixation yields (Fig. 3; Table 4) using the coefficients of the biomass term ($\text{C}_5\text{H}_7\text{O}_2\text{N}$) and N_2 term (Table S1). Figure 3a and b show the amount of biomass produced and N_2 fixed (in mmol) per mol of electron transport. In Fig. 2 and Table S1, all nine overall reactions have a positive coefficient for N_2 as a reactant and biomass as a product, suggesting that the N_2 fixation reaction (Rn) and biosynthesis (Rc) can be performed by all nine of these model organisms.

The significance of this finding is to identify and compare the diverse metabolic pathways that may support N_2 fixation in sedimentary systems with varied nutrient availability. Based on the availability of various electron donors and acceptors in the sediments, our research suggests the potential microbial metabolic pathways that can maintain N_2 fixation under a range of biogeochemical conditions. These models have broader implications that N_2 -fixing communities may be highly flexible with various possible metabolic pathways, which can be adapted to changing environments. Furthermore, this model provides the basic framework for understanding nutrient cycling and microbial ecology in sedimentary environments and other environments inhabited by chemoautotrophic N_2 fixers.

The trend of N_2 fixation yield (Fig. 3b) in different organisms is similar to the biomass yield (Fig. 3a). This is because if more energy and electrons can be provided to biosynthesis, based on the constant fraction of biosynthesis and N_2 fixation in synthesis reactions (equations 15 and 16), more energy and electrons can also be transported to N_2 fixation, causing a higher N_2 fixation yield. In the following sections, we divided the nine organisms into high-efficiency groups (yield higher biomass and N_2 fixation, including methanotrophs [O_2], methanotrophs [NO_3^-], methanotrophs [Fe^{3+}], and all modeled sulfide oxidizers) and low-efficiency groups (yield lower biomass and N_2 fixation, including methanogens and methanotrophs [SO_4^{2-}]).

High-efficiency N_2 fixers

When using the same electron acceptors, methanotrophs can form more biomass (methanotrophs [O_2]: 22.81 mmol/mol e^- , methanotrophs [NO_3^-]: 17.07 mmol/mol e^- , methanotrophs [Fe^{3+}]: 22.35 mmol/mol e^-) and fix more N_2 (methanotrophs [O_2]: 11.41 mmol/mol e^- , methanotrophs [NO_3^-]: 8.534 mmol/mol e^- , methanotrophs [Fe^{3+}]: 11.18 mmol/mol e^-) than sulfide oxidizers (biomass: sulfide oxidizers [O_2]: 21.76 mmol/mol e^- , sulfide oxidizers [NO_3^-]: 15.85 mmol/mol e^- , sulfide oxidizers [Fe^{3+}]: 21.28 mmol/mol e^- ; N_2 fixation: sulfide oxidizers [O_2]: 10.88 mmol/mol e^- , sulfide oxidizers [NO_3^-]: 7.927 mmol/mol e^- , sulfide oxidizers [Fe^{3+}]: 10.64 mmol/mol e^-). For these two different electron donors, methane oxidation ($\Delta G^0 = -23.52 \text{ kJ/e}^- \text{eq}$)

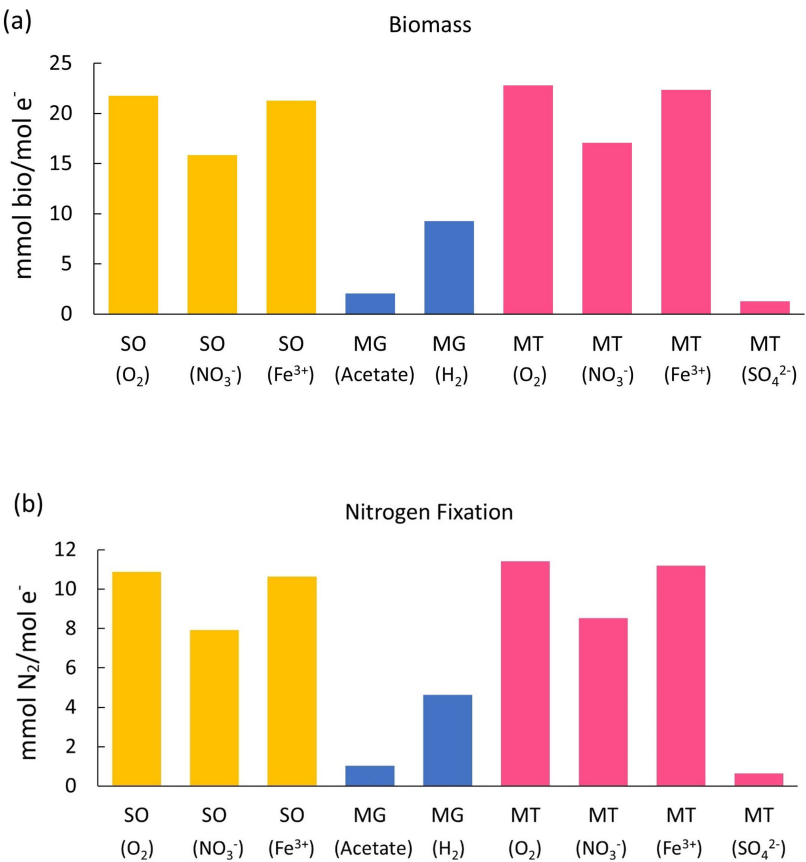


FIG 3 Biomass formation (a) and N₂ fixation (b) comparison. Yellow bars represent sulfide oxidizers (SO) results, blue bars are the methanogens (MG) results, and pink bars are methanotrophs (MT) results.

releases more energy than sulfide oxidation ($\Delta G^{0'} = -20.85 \text{ kJ/e}^- \text{eq}$), supporting more N₂ fixation and growth. Previous studies have found that sulfide oxidizers and N₂ fixers in aquatic systems and sediment (36, 45), with the electron acceptors O₂ and NO₃⁻. Although we haven't found an experimental comparison in N₂ fixation yield between sulfide oxidizers and methanotrophs, our study calculated these theoretical values and fills the gap.

We can also compare the yields among models with different electron acceptors. In our results, O₂ is the best electron acceptor yielding more biomass (Fig. 3a; Table 4, sulfide oxidizer [O₂]: 21.76 mmol/mol e⁻, methanotrophs [O₂]: 22.81 mmol/mol e⁻) and fixing more N₂ (Fig. 3b; Table 4, sulfide oxidizer [O₂]: 10.88 mmol/mol e⁻, methanotroph [O₂]: 11.41 mmol/mol e⁻) than other electron acceptor models. According to the

TABLE 4 Models, electron donors and acceptors, metabolic pathways, and yield

Model	e ⁻ donor	e ⁻ acceptor	Metabolic pathway	Biomass yield (mmol bio/mol e ⁻)	N ₂ fixation yield (mmol N ₂ /mol e ⁻)
Sulfide oxidizer (O ₂)	H ₂ S	O ₂	Oxygenic sulfide oxidation	21.76	10.88
Sulfide oxidizer (NO ₃ ⁻)	H ₂ S	NO ₃ ⁻	Anaerobic sulfide oxidation	15.85	7.927
Sulfide oxidizer (Fe ³⁺)	H ₂ S	Fe ³⁺	Anaerobic sulfide oxidation	21.28	10.64
Methanogen (acetate)	Acetate	CO ₂	Methanogenesis	2.053	1.027
Methanogen (H ₂)	H ₂	CO ₂	Methanogenesis	9.261	4.631
Methanotroph (O ₂)	CH ₄	O ₂	Aerobic methane oxidation	22.81	11.41
Methanotroph (NO ₃ ⁻)	CH ₄	NO ₃ ⁻	Anaerobic methane oxidation	17.07	8.534
Methanotroph (Fe ³⁺)	CH ₄	Fe ³⁺	Anaerobic methane oxidation	22.35	11.18
Methanotroph (SO ₄ ²⁻)	CH ₄	SO ₄ ²⁻	Anaerobic methane oxidation	1.276	0.638

energy state of reactions, O_2 reduction releases more energy ($\Delta G^{0'} = -78.72 \text{ kJ/e}^- \text{eq}$) per electron transport, which provides more energy for growth and N_2 fixation. These efficient aerobic N_2 fixers have been found in soil (49) and fish gills (45). Our models can be used to predict the metabolic pathways, biomass, and N_2 fixation yield of these organisms.

Low-efficiency N_2 fixers

In our simulation results (Table S1), N_2 fixation can be performed by all nine of these model organisms, including some less efficient N_2 fixers, e.g., methanotrophs (SO_4^{2-}). Figure 3 shows that SO_4^{2-} is a less effective acceptor, which can only form 1.276 mmol bio/mol e^- and fix 0.638 mmol N_2 /mol e^- . Although it is less favorable ($\Delta G^{0'} = 20.85 \text{ kJ/e}^- \text{eq}$), it can still happen mathematically, which provides a quantitative explanation for the existence of SO_4^{2-} reduction in methanotrophs. This result is also consistent with field studies, which show that methanotrophic sulfate reducers exist (35) and can inhabit the sulfate–methane interface. In a recent study in cold seeps, researchers found that sulfate reducers could utilize anaerobic methane oxidation to support N_2 fixation (51).

Methanogens (acetate) can form less biomass (2.053 mmol bio/mol e^-) and fix less N_2 (1.027 mmol N_2 /mol e^-) than most other modeled metabolic organisms, except for methanotrophs (SO_4^{2-}) (Fig. 3; Table 4, 1.276 mmol bio/mol e^- and 0.638 mmol N_2 /mol e^-). Methanogens (H_2) have a higher yield in biomass (9.261 mmol bio/mol e^-) and N_2 fixation (4.631 mmol N_2 /mol e^-) than methanogens (acetate), which is because H_2 oxidation is more favorable ($\Delta G^{0'} = -39.87 \text{ kJ/e}^- \text{eq}$) and can provide more energy than methane oxidation. As a result, methanogens (H_2) are more effective than methanogens (acetate). Previous studies in soil have found the *nif* gene in these two methanogens, contributing to the N production in the system (48). In their experiment, researchers found that the addition of H_2 and CO_2 could increase the nitrogenase activity and methane production significantly, while the addition of acetate did not have a significant effect, which is consistent with our model that H_2 is a better electron donor in methanogen N_2 fixers. Researchers also found that these N_2 -fixing methanogen strains can exist in some O_2 -limited environments, including marine sediments and paddy soil (52). In the methanogen (acetate) and methanotroph (SO_4^{2-}) models, Ra and Rd release less energy, leading to higher electron allocation to Ra to provide more energy and a lower allocation to Rc and Rn, resulting in less fixed N_2 and growth.

Effect of pH and temperature

Temperature and pH are both important in biochemical reactions because they directly affect reaction rates and enzyme activity. Higher temperature increases the movement and collision frequency, raising the chance of reactants overcoming the activation energy barrier. Higher temperatures can also provide more energy for N_2 fixation and biosynthesis, facilitating the processes of these reactions. pH can affect chemical reactions directly and modulate enzyme activities. In our model, we tested the effects of temperature and pH (Fig. 4), and we found that in most of the modeled organisms, with the increase in temperature and pH, the N_2 fixation yield increased. This trend may be explained by Le Chatelier's principle (53): when a system's equilibrium is disturbed, it adjusts to counteract the change and restore equilibrium. In the overall reactions for sulfide oxidizers, methanogens, and methanotrophs (Fe^{3+}) (Table S1), since H^+ is on the product side of the overall reactions, decreasing H^+ (higher pH) drives the reaction forward to produce more H^+ , facilitating the overall reactions and fixing more N_2 and growing more biomass. For the methanotrophs (O_2 and NO_3^-), although H^+ occurs on the reactant side of the overall reactions, H^+ could inhibit methane-producing processes, which are the key electron donation processes to support N_2 fixation. For methanotrophs (SO_4^{2-}), decreased pH can facilitate their N_2 fixation because H^+ occurs on the reactant side of their overall reaction.

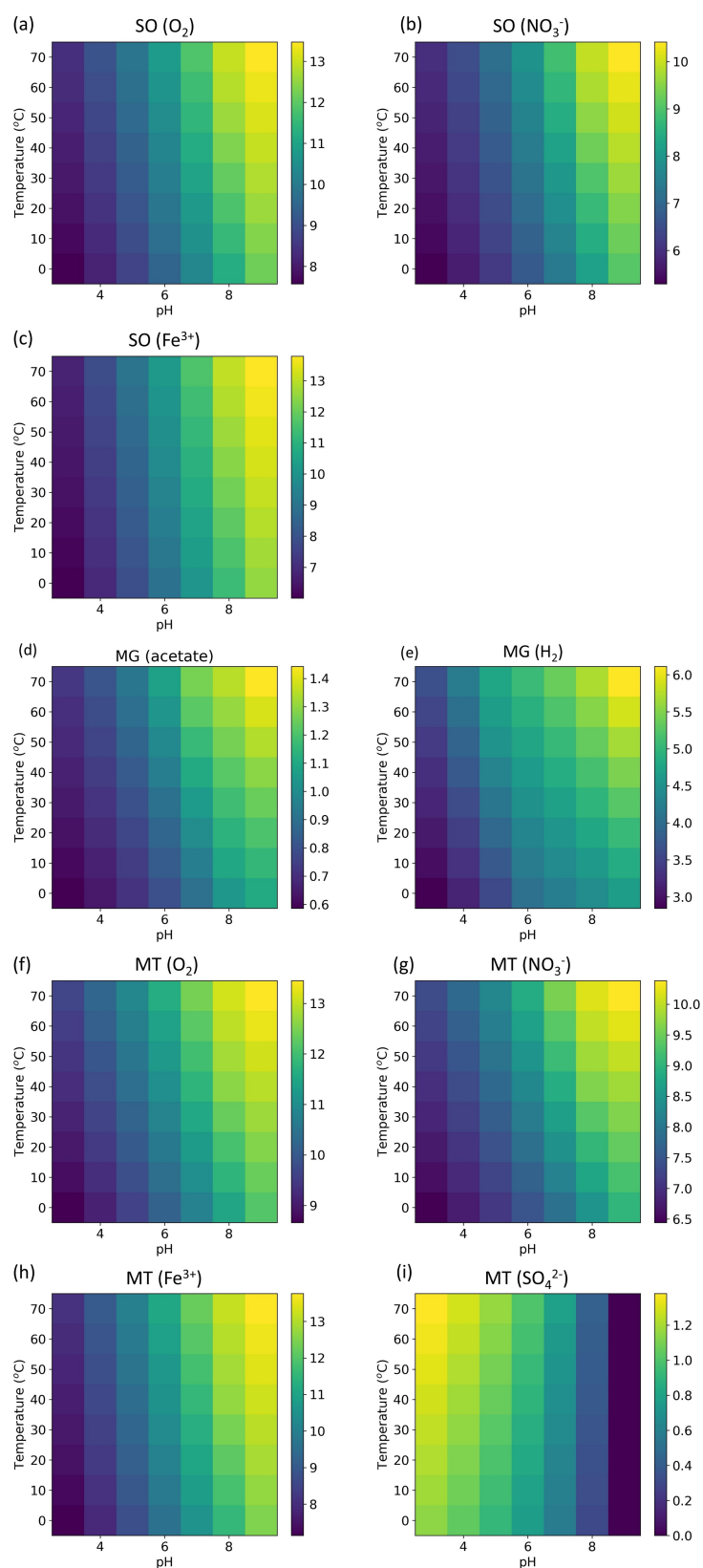


FIG 4 The effect of pH and temperature on N_2 fixation yield (unit: $\text{mmol N}_2/\text{mol e}^-$) for different N_2 fixers (sulfide oxidizers [SO] using O_2 (a), NO_3^- (b), and Fe^{3+} (c); methanogens [MG] using acetate (d) and H_2 (e); Methanotrophs [MT] using O_2 (f), NO_3^- (g), Fe^{3+} (h), and SO_4^{2-} (i)). Color means the N_2 fixation yield ($\text{mol N}_2/\text{mol e}^-$).

Comparison with previous studies: empirical evidence of N₂ fixation for sulfide oxidizers, methanogens, and methanotrophs

Our predictive models based on physical, biochemical, and mathematical principles showed that N₂ fixation could occur alongside biosynthesis in all nine organisms analyzed in this study. Our theoretical findings are supported by previous studies using empirical techniques with varying confidence levels to examine these potential reactions in different habitats. For example, research on sulfide oxidizers in fish gills identified bacteria in the genus *Candidatus* Thiodiazotropha, an aerobic symbiont with the *nif* gene for N₂ fixation (45), which could be applied to our model for sulfide oxidizers (O₂). Additionally, in cold seep ecosystems, researchers found that *Dechloromonas* sp. carried genes related to N₂ fixation (*nifD*HK), sulfur compound oxidation (*fccAB* and *soxABCXYZ*), and nitrate reduction (*napAB* and *nirBD*) (54), which could be applied to the sulfide oxidizer (NO₃[−]) model. Some N₂ fixers, such as *Thiobacillus ferrooxidans*, a sulfide oxidizer living in low pH habitats, were found to fix N₂ (55, 56) and, in some cases, reduce Fe³⁺ (57), which may be related to our sulfide oxidizer (Fe³⁺) models.

For methanotrophs, N₂ fixation can also be confirmed based on N isotope (26, 50) and genetic analysis (49). Auman found that aerobic methanotrophs, *Methylococcus* spp., and sulfide-reducing methanotrophs, *Methylosinus* spp., from soils can fix N₂ (49). Dekas et al. observed that seep N₂ fixation is methane-dependent, and that N₂ fixation rates peak in narrow sediments because of anaerobic methanotrophic archaea and sulfate-reducing bacteria, which form symbionts and fuel the complex ecosystems (58). Cui et al. (26) found that nitrate-reducing methanotrophs, *Methylocystis* spp., in wetlands can fix N₂. In paddy soil under hypoxia, Yu et al. (59) found that methane oxidation coupled with iron reduction can significantly increase the biological N₂ fixation rate, which can happen in *Methylocystis*, *Methylophilaceae*, and *Methylobacterium*. The evidence above can, respectively, fit models of methanotroph (O₂), methanotroph (SO₄^{2−}), methanotroph (NO₃[−]), and methanotroph (Fe³⁺).

Methanogens (*Methanococcus maripaludis* and *Methanococcus thermolithotrophicus*, oxidizing H₂) in lab studies without N-amended media suggested fixed N₂ was the sole N source (60), which is consistent with our methanogen (H₂) model. Genetic analysis also shows that methanogens can fix N₂ (61), for example, in a wetland soil incubation study, researchers found that methanogens using H₂ and acetate both contain N₂ fixation genes (*nifH*) (48), which confirms our findings. All these organisms and symbionts we listed above are commonly active in many aquatic and terrestrial ecosystems, particularly in locations with oxygen gradients or highly anoxic environments, for example, sulfide oxidizers in the redoxcline of the Black Sea (62) and methanogens in marine sediments (63).

Model construction and comparison with different model types

Our model is a coarse-grained model (4), including some important biochemical processes inside the cells. Our model integrates both the sources and utilization of electrons and energy, focusing on two fundamental cellular processes in nitrogen-fixing organisms: N₂ fixation and growth. This modeling framework is adapted from Rittmann and McCarty (47) and follows fundamental mass, electron, and energy conservation principles. For example, when considering half-reactions, we ensure that the energy-providing reactions provide sufficient energy for the overall process to proceed spontaneously. As for electron transport, the model includes both electron donors and acceptors. Various acceptance reactions include energy generation, biomass growth, and N₂ fixation. Additionally, the model ensures that the mass of all chemical elements involved is conserved throughout the reactions.

Our coarse-grained model lies between simple equation models and detailed metabolic models. Different modeling approaches vary in detail and scope, each with strengths and limitations suited to specific applications. Detailed metabolic models can include numerous reactions based on omics data (64). However, they typically require constraints that are often difficult to validate (65–68). On the other end, highly simplified

models like Monod kinetics (69) are highly empirical yet may lack mechanistic processes (70). Coarse-grained models offer a middle-ground solution by resolving key physiological processes while remaining practical, flexible, and empirical (71).

In this study, we chose a coarse-grained model because it focuses on key cellular processes—such as electron donation and acceptance, and the budgets of mass, electrons, and energy—without relying on sets of poorly constrained parameters. We built our models upon an established method of electron allocation, which has been developed by experimental evidence (47). Although there is a possibility of increasing the detail, our level of simplification is deliberate and helps maintain consistency with available empirical data. It also improves computational efficiency and makes the model more broadly applicable across different organisms and environments. This model also provides a single solution rather than multiple possible outcomes, as often seen in more complex approaches like flux balance analysis. By aligning model complexity with data availability, we aim to keep our framework both reliable and widely usable, building on the success of similar approaches in previous studies in both Inomura groups (4, 14, 17, 19, 72) and other groups (6, 73–75).

Future research

Temporal dynamics

Our model begins with steady-state conditions instead of temporal dynamics. Because we are aiming at a steady sedimentary environment, where conditions do not change significantly on the time scale of minutes and hours. The steady-state assumption has been made in multiple previously published models, including most of the detailed metabolic networks (21, 22, 76), and our study followed these examples. Regardless, future research may resolve temporal dynamics to explore the shift in chemoautotrophic N_2 fixation in a longer time series.

Depth distribution

Our models help to clarify the theoretical biochemical principles behind N_2 fixation metabolism, which can be used to understand the spatial ecological niche of various chemoautotrophic N_2 fixers. The availability and favorability of the reduction of the electron acceptors may interact to create a depth distribution of different N_2 fixers along oxic-anoxic gradients in sediments. For example, NO_3^- reduction is more favorable than SO_4^{2-} reduction, resulting in NO_3^- reducers being found in the upper layer of the sediment (77, 78). In river estuarine sediments, SO_4^{2-} reduction was also reported to have a potential relationship with N_2 fixation (79). Specifically, sampling from different sediment depths combined with transcriptomics and proteomics could further validate and expand our modeling results.

Conclusions

We constructed a whole-cell reaction stoichiometry of putative chemoautotrophic N_2 -fixing organisms. The results show a range of electron allocation based on the energetics of the half-reactions. All these putative metabolic organisms allow N_2 fixation and biosynthesis to occur, and thus, our work uncovers the potential reactions coupled with N_2 fixation. Based on the electron allocation results, O_2 is a better electron acceptor because chemotrophs using O_2 can allocate more electrons to N_2 fixation and growth. From the biomass and N_2 fixation yield, we found that aerobic N_2 fixers are more efficient, while SO_4^{2-} reducers and methanogens (acetate) are less efficient. However, even less favorable substrates, SO_4^{2-} and CH_4 , can support N_2 fixation. The variation between different organisms allows for the consumption of various substrates in the different catabolic reactions supporting N_2 fixation, which may occur at different oxidative/reductive environments in aquatic systems at different depths. It is challenging to precisely measure the metabolisms of microorganisms living in sediments under variable environmental conditions. Therefore, our model will be useful in investigating

the likely depth-dependent metabolic pathways for different substrate compositions. These predictions can complement field measurements by providing estimates of the contribution of chemoautotrophs to N_2 fixation.

MATERIALS AND METHODS

Our CFM-CNF follows an original cell flux model (CFM) structure, which simulates *Azotobacter vinelandii* (17), an extensively studied soil-dwelling N_2 fixer. We targeted organisms inhabiting sediments, where O_2 concentrations are typically low. So, we assume that the O_2 concentration is low enough that we can neglect the protection from O_2 (i.e., the respiratory protection), especially for those anaerobes using non-oxygen substrates for electron acceptors living in anoxic environments. Since we did not target the heterotrophic organisms living in highly oxic environments (e.g., those in water columns), we did not include O_2 inhibition in this model.

This model summarizes the cell metabolism and combines four biochemical reactions: electron donation (Rd), electron acceptance for non-synthesis purposes such as energy generation (Ra), biosynthesis (Rc), and N_2 fixation (Rn). This model can be used to calculate electron flow, biomass, and N_2 fixation yield. Here, we explained the calculation method step by step.

Energy reactions

Microorganisms obtain their energy for growth and maintenance from oxidation-reduction reactions, involving an electron donation half-reaction (Rd) and an electron acceptance half-reaction (Ra). For different potential N_2 fixers in this study, we used different Rd and Ra (Table 1). We listed the Gibbs free energy change ($\Delta G^{0'}$) for different Rd and Ra (Table S5), which describes their favorability under standard conditions. Based on their energy change, we then decide the energy-providing reactions and potential energy flow within the model.

Biosynthesis reactions

Bacterial metabolic pathways involve two types of basic reactions, one for energy (mentioned in the last section) and the other for cellular synthesis (e.g., growth and maintenance). In this step, we need to consider the half-reactions for the synthesis part. For the growth of cells (Rc), we used equation 11. Since the purpose of this study is to model N_2 fixers, here we also consider N_2 fixation as a part of the maintenance of the cell (equation 1).

Electron allocation

When microorganisms use an electron-donor substrate for synthesis, a portion of their electrons (f_e) is initially transferred to the electron acceptor to provide energy. Other portions of electrons can be transferred to growth and maintenance (f_s). The sum of f_e and f_s is 1 since we assumed one electron was transferred in this study.

Then, we calculated the allocation of electrons following the method in reference 47 (equations 12 to 14). Firstly, we calculated a parameter A (equation 12, derivation in the supplemental material) representing the number of electron donors that must be oxidized to supply the energy needed for cell synthesis. In equation 12, ΔG_n means Gibbs free energy change for N_2 fixation, ΔG_p means the energy required to convert the carbon source to the common organic intermediates (activated acetate) that cells use for synthesizing their macromolecules, and ΔG_{pc} means the energy used to convert the organic intermediates to cellular carbon. We used $18.8 \text{ kJ/e}^- \text{ eq}$ as ΔG_{pc} . ε is energy transfer efficiency. Rittmann and McCarty (47) reported that with the optimum conditions, transfer efficiencies of 55% to 70% are typical for most anaerobic and

chemoautotrophic reactions, and a ε value of 0.6 is frequently employed to provide accurate results. So here we used ε equals to 0.6 for all the chemoautotrophs.

Here, an exponent n is used for the calculation of ε , according to Rittmann and McCarty (47), if ΔG_p is positive, n is 1; if ΔG_p is negative, n is -1 . ΔG_r was calculated by using Gibbs free energy change for the electron acceptance reaction (Ra) and Gibbs free energy change in the electron donation reaction (Rd).

$$A = - \frac{\left(f_n \times \Delta G_n + f_c \times \left(\frac{\Delta G_p}{\varepsilon^n} + \frac{\Delta G_{pc}}{\varepsilon}\right)\right)}{\varepsilon \Delta G_r}. \quad (12)$$

We used the A value to calculate electron allocation to cell synthesis (equation 13, f_s , including Rc and Rn) and energy production (equation 14, f_e). The derivation of equation 13 and equation 14 is in the supplemental material (equations S7 to S12).

$$f_s = \frac{1}{1 + A} \quad (13)$$

$$f_e = \frac{A}{1 + A} \quad (14)$$

Here, we explain the equations we used to calculate the fraction of biosynthesis and N_2 fixation. In equation 15, f_c means the fraction of electrons allocated to Rc over the total electrons allocated to Rc and Rn. $Y_{\text{bio}}^{\text{e}^-:\text{N}}$ means the transferred electrons to biomass N ratio in Rc, and $Y_{\text{N}_2\text{fix}}^{\text{e}^-:\text{N}}$ means the transferred electrons to fixed N ratio in Rn. We calculated the ratio of Rc ($Y_{\text{bio}}^{\text{e}^-:\text{N}}$) to the sum of Rc and Rn ($Y_{\text{bio}}^{\text{e}^-:\text{N}} + Y_{\text{N}_2\text{fix}}^{\text{e}^-:\text{N}}$) to obtain this electron allocation fraction of Rc (f_c). In equation 16, the calculation is similar; we calculated this fraction of Rn (f_n) out of the sum of Rn and Rc by using the electron ratio of Rn ($Y_{\text{N}_2\text{fix}}^{\text{e}^-:\text{N}}$) to the sum of Rc and Rn ($Y_{\text{bio}}^{\text{e}^-:\text{N}} + Y_{\text{N}_2\text{fix}}^{\text{e}^-:\text{N}}$).

$$f_c = \frac{Y_{\text{bio}}^{\text{e}^-:\text{N}}}{Y_{\text{bio}}^{\text{e}^-:\text{N}} + Y_{\text{N}_2\text{fix}}^{\text{e}^-:\text{N}}} \quad (15)$$

$$f_n = \frac{Y_{\text{N}_2\text{fix}}^{\text{e}^-:\text{N}}}{Y_{\text{bio}}^{\text{e}^-:\text{N}} + Y_{\text{N}_2\text{fix}}^{\text{e}^-:\text{N}}} \quad (16)$$

Overall reactions and yield calculation

The mass is conserved in each half-reaction. We combine these reactions to balance electrons and energy. In all the cases in this study, the combination of Rd and Ra leads to energy production, which is, in turn, used for biosynthesis (Rc) and N_2 fixation (Rn).

Equation 17 shows the calculation of R_e (the overall reactions for energy). It can be calculated from the difference between Ra and Rd.

$$R_e = R_a - R_d \quad (17)$$

The synthesis reactions (R_s) (equation 18) are calculated from the difference between synthesis half reactions (Rsh) and donation (Rd).

$$R_s = R_{sh} - R_d \quad (18)$$

Here, we considered Rn and Rc as two different sections of the synthesis half reactions (Rsh). To calculate Rsh, we multiplied Rc by a fraction of Rc (f_c) as the biosynthesis section. We multiplied Rn by a fraction of Rn (f_n) as the N_2 fixation section.

$$R_{sh} = f_c R_c + f_n R_n \quad (19)$$

Then we substitute R_{sh} into equation 18, yielding equation 20.

$$R_s = f_c R_c + f_n R_n - R_d \quad (20)$$

Finally, we estimated the overall reaction, which is the sum of energy reactions (R_e) and synthesis reactions (R_s). Here, we calculated this by using equation 21. We multiplied R_e by the electron fractions to energy (f_e) and R_s by the electron fractions to synthesis (f_s).

$$R = f_e \times R_e + f_s \times R_s \quad (21)$$

We finally substituting equations 18 and 20 into equation 21 yields the final equation, and calculated the overall reactions (equation 22). The overall reactions for different modeling organisms are presented in Table S1. Based on the coefficients of the overall reactions, we can compare the yield for N_2 fixation and biosynthesis. The coefficients before the N_2 term mean the N_2 fixed per electron, while the coefficients before the biomass term mean the biomass produced per electron.

$$R = f_e \times (R_a - R_d) + f_s \times (f_c R_c + f_n R_n - R_d) \quad (22)$$

The specific values we used to do the calculations (Table S3) are all from Rittmann and McCarty (47). For different models, we have different values, which have been listed in the supplementary parameter tables (Tables S3 through S6).

ACKNOWLEDGMENTS

We thank the Aquatic Nitrogen Fixation Research Coordination Network (RCN) for support and contributions to this work. RCN was supported by the U.S. National Science Foundation (NSF) under Award No. DEB-2015825 (J.T.S., A.M.M., R.W.F.). This project was also supported by the Simons Foundation (LS-ECIAMEE-00001549, K.I.), the NSF under Award No. OCE-2227425 (K.I.), DEB-1943182 (D.M.C.), OCE-2048373 (subaward SUB0000525 from Princeton University, K. I.), and “Ramón y Cajal” Fellowship (RYC2022-036661-I) from the Spanish Ministry of Science (A.P.), and we are grateful for their support.

AUTHOR AFFILIATIONS

¹Graduate School of Oceanography, University of Rhode Island, Narragansett, Rhode Island, USA

²Department of Biological Sciences, Michigan Technological University, Houghton, Michigan, USA

³Department of Plant and Microbial Biology, University of Minnesota-Twin Cities, Saint Paul, Minnesota, USA

⁴Department of Biological Sciences, Kent State University, Kent, Ohio, USA

⁵Department of Ecology, Evolution and Behavior, University of Minnesota-Twin Cities, Saint Paul, Minnesota, USA

⁶University of Bergen, Bergen, Norway

⁷Department of Biology, Hamilton College, Clinton, New York, USA

⁸GEOMAR Helmholtz Centre for Ocean Research, Kiel, Germany

⁹Group of Continental Aquatic Ecology Research (GRECO), Institute of Aquatic Ecology, Universitat de Girona, Girona, Spain

¹⁰Departments of Earth & Environment and Biology, Boston University, Boston, Massachusetts, USA

¹¹Department of Biology, Baylor University, Waco, Texas, USA

AUTHOR ORCID*s*

Meng Gao [id](http://orcid.org/0009-0008-8017-4436) <http://orcid.org/0009-0008-8017-4436>
 Megan E. Berberich [id](http://orcid.org/0000-0001-5363-892X) <http://orcid.org/0000-0001-5363-892X>
 Reid Brown [id](http://orcid.org/0000-0003-1424-9926) <http://orcid.org/0000-0003-1424-9926>
 David M. Costello [id](http://orcid.org/0000-0002-1532-5399) <http://orcid.org/0000-0002-1532-5399>
 James B. Cotner [id](http://orcid.org/0000-0001-9792-467X) <http://orcid.org/0000-0001-9792-467X>
 Julian Damashek [id](https://orcid.org/0000-0001-5778-0157) <https://orcid.org/0000-0001-5778-0157>
 Leila Richards Kittu [id](http://orcid.org/0000-0002-3986-8179) <http://orcid.org/0000-0002-3986-8179>
 Ada Pastor [id](http://orcid.org/0000-0002-7114-770X) <http://orcid.org/0000-0002-7114-770X>
 Robinson W. Fulweiler [id](http://orcid.org/0000-0003-0871-4246) <http://orcid.org/0000-0003-0871-4246>
 J. Thad Scott [id](http://orcid.org/0000-0002-9487-9698) <http://orcid.org/0000-0002-9487-9698>
 Amy M. Marcarelli [id](http://orcid.org/0000-0002-4175-9211) <http://orcid.org/0000-0002-4175-9211>
 Keisuke Inomura [id](http://orcid.org/0000-0001-9232-7032) <http://orcid.org/0000-0001-9232-7032>

FUNDING

Funder	Grant(s)	Author(s)
U.S. National Science Foundation	OCE-2227425	Keisuke Inomura
U.S. National Science Foundation, (subaward SUB0000525 from Princeton University)	OCE-2048373	Keisuke Inomura
Simons Foundation	LS-ECIAMEE-00001549	Keisuke Inomura
U.S. National Science Foundation	DEB-2015825	J. Thad Scott Amy M. Marcarelli Robinson W. Fulweiler
Spanish Ministry of Science, Ramón y Cajal Fellowship	RYC2022-036661-I	Ada Pastor
U.S. National Science Foundation	DEB-1943182	David M. Costello

DATA AVAILABILITY

The data sets generated and/or analyzed during the current study are available in the "Biochemical model for sediment N₂ fixers" repository at <https://doi.org/10.5281/zenodo.12680697>.

ADDITIONAL FILES

The following material is available [online](#).

Supplemental Material

Supplemental Material (mSystems00748-25-S0001.pdf). Tables S1 to S6; Fig. S1.

REFERENCES

- Gruber N, Galloway JN. 2008. An Earth-system perspective of the global nitrogen cycle. *Nature* 451:293–296. <https://doi.org/10.1038/nature06592>
- Sohm JA, Webb EA, Capone DG. 2011. Emerging patterns of marine nitrogen fixation. *Nat Rev Microbiol* 9:499–508. <https://doi.org/10.1038/nrmicro2594>
- Vitousek PM, Cassman K, Cleveland C, Crews T, Field CB, Grimm NB, Howarth RW, Marino R, Martinelli L, Rastetter EB, Sprent JI. 2002. Towards an ecological understanding of biological nitrogen fixation. *Biogeochemistry* 57–58:1–45. <https://doi.org/10.1023/A:1015798428743>
- Inomura K, Deutsch C, Masuda T, Prášil O, Follows MJ. 2020. Quantitative models of nitrogen-fixing organisms. *Comput Struct Biotechnol J* 18:3905–3924. <https://doi.org/10.1016/j.csbj.2020.11.022>
- Zehr JP, Capone DG. 2020. Changing perspectives in marine nitrogen fixation. *Science* 368:eaay9514. <https://doi.org/10.1126/science.aay9514>
- Chakraborty S, Andersen KH, Visser AW, Inomura K, Follows MJ, Riemann L. 2021. Quantifying nitrogen fixation by heterotrophic bacteria in sinking marine particles. *Nat Commun* 12:4085. <https://doi.org/10.1038/s41467-021-23875-6>
- Zehr JP. 2011. Nitrogen fixation by marine cyanobacteria. *Trends Microbiol* 19:162–173. <https://doi.org/10.1016/j.tim.2010.12.004>
- Benavides M, Bonnet S, Berman-Frank I, Riemann L. 2018. Deep into oceanic N₂ fixation. *Front Mar Sci* 5. <https://doi.org/10.3389/fmars.2018.00108>
- Mulholland MR, Bernhardt PW, Widner BN, Selden CR, Chappell PD, Clayton S, Mannino A, Hyde K. 2019. High rates of N₂ fixation in temperate, Western North Atlantic coastal waters expand the realm of

- marine diazotrophy. *Global Biogeochem Cycles* 33:826–840. <https://doi.org/10.1029/2018GB006130>
10. Blais M, Tremblay JÉ, Jungblut AD, Gagnon J, Martin J, Thaler M, Lovejoy C. 2012. Nitrogen fixation and identification of potential diazotrophs in the Canadian Arctic. *Global Biogeochem Cycles* 26. <https://doi.org/10.1029/2011GB004096>
 11. von Friesen LW, Riemann L. 2020. Nitrogen fixation in a changing Arctic Ocean: an overlooked source of nitrogen? *Front Microbiol* 11:596426. <https://doi.org/10.3389/fmicb.2020.596426>
 12. Marcarelli AM, Fulweiler RW, Scott JT. 2022. Nitrogen fixation: a poorly understood process along the freshwater-marine continuum. *Limnol Oceanogr Lett* 7:1–10. <https://doi.org/10.1002/lol2.10220>
 13. Fulweiler RW. 2023. More foxes than hedgehogs: the case for nitrogen fixation in coastal marine sediments. *Global Biogeochem Cycles* 37. <https://doi.org/10.1029/2023GB007777>
 14. Inomura K, Wilson ST, Deutsch C. 2019. Mechanistic model for the coexistence of nitrogen fixation and photosynthesis in marine *Trichodesmium*. *mSystems* 4:e00210–19. <https://doi.org/10.1128/mSystems.00210-19>
 15. Inomura K, Deutsch C, Wilson ST, Masuda T, Lawrenz E, Lenka B, Sobotka R, Gauglitz JM, Saito MA, Prášil O, Follows MJ. 2019. Quantifying oxygen management and temperature and light dependencies of nitrogen fixation by *Crocospaera watsonii*. *mSphere* 4:e00531–19. <https://doi.org/10.1128/mSphere.00531-19>
 16. Luo W, Inomura K, Zhang H, Luo Y-W. 2022. N₂ fixation in *Trichodesmium* does not require spatial segregation from photosynthesis. *mSystems* 7:e00538–22. <https://doi.org/10.1128/mSystems.00538-22>
 17. Inomura K, Bragg J, Follows MJ. 2017. A quantitative analysis of the direct and indirect costs of nitrogen fixation: a model based on *Azotobacter vinelandii*. *ISME J* 11:166–175. <https://doi.org/10.1038/ismej.2016.97>
 18. Inomura K, Bragg J, Riemann L, Follows MJ. 2018. A quantitative model of nitrogen fixation in the presence of ammonium. *PLoS One* 13:e0208282. <https://doi.org/10.1371/journal.pone.0208282>
 19. Gao M, Armin G, Inomura K. 2022. Low-ammonium environment increases the nutrient exchange between diatom–diazotroph association cells and facilitates photosynthesis and N₂ fixation—a mechanistic modeling analysis. *Cells* 11:2911. <https://doi.org/10.3390/cells11182911>
 20. Gao M, Andrews J, Armin G, Chakraborty S, Zehr JP, Inomura K. 2024. Rapid model switching facilitates the growth of *Trichodesmium*: a model analysis. *iScience* 27:109906. <https://doi.org/10.1016/j.isci.2024.109906>
 21. Inomura K, Follett CL, Masuda T, Eichner M, Prášil O, Deutsch C. 2020. Carbon transfer from the host diatom enables fast growth and high rate of N₂ fixation by symbiotic heterocystous cyanobacteria. *Plants (Basel)* 9:8–16. <https://doi.org/10.3390/plants9020192>
 22. Inomura K, Omta AW, Talmay D, Bragg J, Deutsch C, Follows MJ. 2020. A mechanistic model of macromolecular allocation, elemental stoichiometry, and growth rate in phytoplankton. *Front Microbiol* 11:86. <https://doi.org/10.3389/fmicb.2020.00086>
 23. Seefeldt LC, Hoffman BM, Dean DR. 2009. Mechanism of molybdenum-dependent nitrogenase. *Annu Rev Biochem* 78:701–722. <https://doi.org/10.1146/annurev.biochem.78.070907.103812>
 24. Chen Y-P, Yoch DC. 1988. Reconstitution of the electron transport system that couples formate oxidation to nitrogenase in *Methylosinus trichosporium* OB3b. *Microbiology (Reading)* 134:3123–3128. <https://doi.org/10.1099/00221287-134-12-3123>
 25. Jungermann K, Kirchner H, Katz N, Thauer RK. 1974. NADH, a physiological electron donor in clostridial nitrogen fixation. *FEBS Lett* 43:203–206. [https://doi.org/10.1016/0014-5793\(74\)81000-8](https://doi.org/10.1016/0014-5793(74)81000-8)
 26. Cui J, Zhang M, Chen L, Zhang S, Luo Y, Cao W, Zhao J, Wang L, Jia Z, Bao Z. 2022. Methanotrophs contribute to nitrogen fixation in emergent Macrophytes. *Front Microbiol* 13:851424. <https://doi.org/10.3389/fmicb.2022.851424>
 27. Kits KD, Campbell DJ, Rosana AR, Stein LY. 2015. Diverse electron sources support denitrification under hypoxia in the obligate methanotroph *Methylobacterium album* strain BG8. *Front Microbiol* 6. <https://doi.org/10.3389/fmicb.2015.01072>
 28. Cai C, Leu AO, Xie G-J, Guo J, Feng Y, Zhao J-X, Tyson GW, Yuan Z, Hu S. 2018. A methanotrophic archaeon couples anaerobic oxidation of methane to Fe(III) reduction. *ISME J* 12:1929–1939. <https://doi.org/10.1038/s41396-018-0109-x>
 29. Yu H, Kennerton CT, Chadwick GL, Leu AO, Aoki M, Tyson GW, Orphan VJ. 2022. Sulfate differentially stimulates but is not respired by diverse anaerobic methanotrophic archaea. *ISME J* 16:168–177. <https://doi.org/10.1038/s41396-021-01047-0>
 30. Guerrero-Cruz S, Vaksmaa A, Horn MA, Niemann H, Pijuan M, Ho A. 2021. Methanotrophs: discoveries, environmental relevance, and a perspective on current and future applications. *Front Microbiol* 12:678057. <https://doi.org/10.3389/fmicb.2021.678057>
 31. Berger S, Shaw DR, Berben T, Ouboter HT, In 't Zandt MH, Frank J, Reimann J, Jetten MSM, Welte CU. 2021. Current production by non-methanotrophic bacteria enriched from an anaerobic methane-oxidizing microbial community. *Biofilm* 3:100054. <https://doi.org/10.1016/j.biofilm.2021.100054>
 32. Conrad R. 1999. Contribution of hydrogen to methane production and control of hydrogen concentrations in methanogenic soils and sediments. *FEMS Microbiol Ecol* 28:193–202. [https://doi.org/10.1016/S0168-6496\(98\)00086-5](https://doi.org/10.1016/S0168-6496(98)00086-5)
 33. Canfield DE, Kristensen E, Thamdrup B. 2005. Aquatic geomicrobiology. *Adv Mar Biol* 48:1–599. [https://doi.org/10.1016/S0065-2881\(05\)48017-7](https://doi.org/10.1016/S0065-2881(05)48017-7)
 34. Leigh JA. 2000. Nitrogen fixation in methanogens. *Curr Issues Mol Biol* 2:125–131. <https://doi.org/10.21775/cimb.002.125>
 35. Siegert M, Taubert M, Seifert J, von Bergen-Tomm M, Basen M, Bastida F, Gehre M, Richnow H-H, Krüger M. 2013. The nitrogen cycle in anaerobic methanotrophic mats of the Black Sea is linked to sulfate reduction and biomass decomposition. *FEMS Microbiol Ecol* 86:231–245. <https://doi.org/10.1111/1574-6941.12156>
 36. Rolando JL, Kolton M, Song T, Liu Y, Pinamang P, Conrad R, Morris JT, Konstantinidis KT, Kostka JE. 2023. Sulfur oxidation and reduction are coupled to nitrogen fixation in the roots of a salt marsh foundation plant species. *bioRxiv*. <https://doi.org/10.1101/2023.05.01.538948>
 37. Henkel JV, Schulz-Vogt HN, Dellwig O, Pollehn F, Schott T, Meeske C, Beier S, Jürgens K. 2022. Biological manganese-dependent sulfide oxidation impacts elemental gradients in redox-stratified systems: indications from the Black Sea water column. *ISME J* 16:1523–1533. <https://doi.org/10.1038/s41396-022-01200-3>
 38. Fan X, Xing X, Ding S. 2021. Enhancing the retention of phosphorus through bacterial oxidation of iron or sulfide in the eutrophic sediments of Lake Taihu. *Sci Total Environ* 791:148039. <https://doi.org/10.1016/j.scitotenv.2021.148039>
 39. Preisler A, de Beer D, Lichtschlag A, Lavik G, Boetius A, Jørgensen BB. 2007. Biological and chemical sulfide oxidation in a *Beggiatoa* inhabited marine sediment. *ISME J* 1:341–353. <https://doi.org/10.1038/ismej.2007.50>
 40. Ende FP, Gernerden H. 1993. Sulfide oxidation under oxygen limitation by a *Thiobacillus thioparus* isolated from a marine microbial mat. *FEMS Microbiol Ecol* 13:69–77. <https://doi.org/10.1111/j.1574-6941.1993.tb00052.x>
 41. Sievert SM, Hügler M, Taylor CD, Wirsén CO. 2008. Sulfur oxidation at deep-sea hydrothermal vents, p 238–258. In Dahl C, Friedrich CG (ed), *Microbial sulfur metabolism*. Springer, Berlin.
 42. Marzocchi A, Trojan D, Larsen S, Meyer RL, Revsbech NP, Schramm A, Nielsen LP, Risgaard-Petersen N. 2014. Electric coupling between distant nitrate reduction and sulfide oxidation in marine sediment. *ISME J* 8:1682–1690. <https://doi.org/10.1038/ismej.2014.19>
 43. Brunet RC, Garcia-Gil LJ. 2006. Sulfide-induced dissimilatory nitrate reduction to ammonia in anaerobic freshwater sediments. *FEMS Microbiol Ecol* 21:131–138. <https://doi.org/10.1111/j.1574-6941.1996.tb00340.x>
 44. Norris PR, Colin Murrell J, Hinson D. 1995. The potential for diazotrophy in iron- and sulfur-oxidizing acidophilic bacteria. *Arch Microbiol* 164:294–300. <https://doi.org/10.1007/BF02529964>
 45. König S, Gros O, Heiden SE, Hinzke T, Thürmer A, Poehlein A, Meyer S, Vatin M, Mbéguié-A-Mbéguié D, Toczny J, Ponnudurai R, Daniel R, Becher D, Schweder T, Markert S. 2016. Nitrogen fixation in a chemolithotrophic lucinid symbiosis. *Nat Microbiol* 2:16193. <https://doi.org/10.1038/nmicrobiol.2016.193>
 46. Gier J, Sommer S, Löscher CR, Dale AW, Schmitz RA, Treude T. 2016. Nitrogen fixation in sediments along a depth transect through the Peruvian oxygen minimum zone. *Biogeosciences* 13:4065–4080. <https://doi.org/10.5194/bg-13-4065-2016>
 47. Rittmann B, McCarty PL. 2020. *Environmental biotechnology: principles and applications*. McGraw-Hill, New York, NY.
 48. Bae HS, Morrison E, Chanton JP, Ogram A. 2018. Methanogens are major contributors to nitrogen fixation in soils of the Florida Everglades. *Appl Environ Microbiol* 84:e02222–17. <https://doi.org/10.1128/AEM.02222-17>

49. Auman AJ, Speake CC, Lidstrom ME. 2001. *nifH* sequences and nitrogen fixation in type I and type II methanotrophs. *Appl Environ Microbiol* 67:4009–4016. <https://doi.org/10.1128/AEM.67.9.4009-4016.2001>
50. Hara S, Wada N, Hsiao SSY, Zhang M, Bao Z, Iizuka Y, Lee DC, Sato S, Tang SL, Minamisawa K. 2022. *In vivo* evidence of single ^{13}C and ^{15}N isotope-labeled methanotrophic nitrogen-fixing bacterial cells in rice roots. *mBio* 13:e01255-22. <https://doi.org/10.1128/mbio.01255-22>
51. Wang X, Zhao D, Yu T, Zhu Y, Jiang M, Liu Y, Hu S, Luo Y, Xiang H, Zheng Y. 2025. Biological nitrogen fixation driven by methane anaerobic oxidation supports the complex biological communities in cold-seep habitat. *Environ Technol Innov* 37:103938. <https://doi.org/10.1016/j.eti.2024.103938>
52. Mo Y, Li J, Peng X, Ho A, Jia Z. 2024. Coupling methane oxidation and N_2 fixation under methanogenic conditions in contrasting environments. *Eur J Soil Biol* 123:103693. <https://doi.org/10.1016/j.ejsobi.2024.103693>
53. Le Chatelier H. 1884. On a general statement of the laws of chemical equilibrium. *C R Acad Sci Paris* 99:786–789.
54. Quan Q, Liu J, Xia X, Zhang S, Ke Z, Wang M, Tan Y. 2024. Cold seep nitrogen fixation and its potential relationship with sulfur cycling. *Microbiol Spectr* 12:e00536-24. <https://doi.org/10.1128/spectrum.00536-24>
55. Mackintosh ME. 1978. Nitrogen fixation by *Thiobacillus ferrooxidans*. *J Gen Microbiol* 105:215–218. <https://doi.org/10.1099/00221287-105-2-215>
56. Yamada S, Suzuki Y, Kouzuma A, Watanabe K. 2022. Development of a CRISPR interference system for selective gene knockdown in *Acidithiobacillus ferrooxidans*. *J Biosci Bioeng* 133:105–109. <https://doi.org/10.1016/j.jbiosc.2021.10.012>
57. Pronk JT, de Bruyn JC, Bos P, Kuenen JG. 1992. Anaerobic growth of *Thiobacillus ferrooxidans*. *Appl Environ Microbiol* 58:2227–2230. <https://doi.org/10.1128/aem.58.7.2227-2230.1992>
58. Dekas AE, Chadwick GL, Bowles MW, Joye SB, Orphan VJ. 2014. Spatial distribution of nitrogen fixation in methane seep sediment and the role of the ANME archaea. *Environ Microbiol* 16:3012–3029. <https://doi.org/10.1111/1462-2920.12247>
59. Yu L, Jia R, Liu S, Li S, Zhong S, Liu G, Zeng RJ, Rensing C, Zhou S. 2024. Ferrihydrite-mediated methanotrophic nitrogen fixation in paddy soil under hypoxia. *ISME Commun* 4:ycae030. <https://doi.org/10.1093/ismeco/ycae030>
60. Belay N, Spading R, Choi B-S, Roberts M, Roberts JE, Daniels L. 1988. Physiological and ^{15}N -NMR analysis of molecular nitrogen fixation by *Methanoeoccus thennolithotrophicus*, *Methanobacterium bryantii* and *Methanospirillum hungatei*. *Biochim Biophys Acta* 971:233–245. [https://doi.org/10.1016/S0005-2728\(88\)80037-9](https://doi.org/10.1016/S0005-2728(88)80037-9)
61. Boyd ES, Anbar AD, Miller S, Hamilton TL, Lavin M, Peters JW. 2011. A late methanogen origin for molybdenum-dependent nitrogenase. *Geobiology* 9:221–232. <https://doi.org/10.1111/j.1472-4669.2011.00278.x>
62. Kirkpatrick JB, Fuchsman CA, Yakushev EV, Egorov AV, Staley JT, Murray JW. 2018. Dark N_2 fixation: *nifH* expression in the redoxcline of the Black Sea. *Aquat Microb Ecol* 82:43–58. <https://doi.org/10.3354/ame01882>
63. Ferry JG, Lessner DJ. 2008. Methanogenesis in marine sediments. *Ann N Y Acad Sci* 1125:147–157. <https://doi.org/10.1196/annals.1419.007>
64. Orth JD, Thiele I, Palsson BØ. 2010. What is flux balance analysis? *Nat Biotechnol* 28:245–248. <https://doi.org/10.1038/nbt.1614>
65. Morales Y, Tortajada M, Picó J, Vehí J, Llaneras F. 2014. Validation of an FBA model for *Pichia pastoris* in chemostat cultures. *BMC Syst Biol* 8:142. <https://doi.org/10.1186/s12918-014-0142-y>
66. Kaste JAM, Shachar-Hill Y. 2024. Model validation and selection in metabolic flux analysis and flux balance analysis. *Biotechnol Prog* 40:e3413. <https://doi.org/10.1002/btpr.3413>
67. Sen P. 2024. Flux balance analysis of metabolic networks for efficient engineering of microbial cell factories. *Biotechnol Genet Eng Rev* 40:3682–3715. <https://doi.org/10.1080/02648725.2022.2152631>
68. Raman K, Chandra N. 2009. Flux balance analysis of biological systems: applications and challenges. *Brief Bioinform* 10:435–449. <https://doi.org/10.1093/bib/bbp011>
69. Monod J. 1949. The growth of bacterial cultures. *Annu Rev Microbiol* 3:371–394. <https://doi.org/10.1146/annurev.mi.03.100149.002103>
70. Armin G, Kim J, Inomura K. 2023. Saturating growth rate against phosphorus concentration explained by macromolecular allocation. *mSystems* 8:e00611-23. <https://doi.org/10.1128/msystems.00611-23>
71. Follows MJ, Dutkiewicz S. 2011. Modeling diverse communities of marine microbes. *Ann Rev Mar Sci* 3:427–451. <https://doi.org/10.1146/annurev-marine-120709-142848>
72. Armin G, Inomura K. 2021. Modeled temperature dependencies of macromolecular allocation and elemental stoichiometry in phytoplankton. *Comput Struct Biotechnol J* 19:5421–5427. <https://doi.org/10.1016/j.csbj.2021.09.028>
73. Leles SG, Levine NM. 2023. Mechanistic constraints on the trade-off between photosynthesis and respiration in response to warming. *Sci Adv* 9:eadh8043. <https://doi.org/10.1126/sciadv.adh8043>
74. Chakraborty S, Andersen KH, Merico A, Riemann L. 2025. Particle-associated N_2 fixation by heterotrophic bacteria in the global ocean. *Sci Adv* 11:eadq4693. <https://doi.org/10.1126/sciadv.adq4693>
75. Geider RJ, MacIntyre HL, Kana TM. 1998. A dynamic regulatory model of phytoplankton acclimation to light, nutrients, and temperature. *Limnol Oceanogr* 43:679–694. <https://doi.org/10.4319/lo.1998.43.4.0679>
76. Inomura K, Masuda T, Gauglitz JM. 2019. Active nitrogen fixation by *Crocospaera* expands their niche despite the presence of ammonium - a case study. *Sci Rep* 9:15064. <https://doi.org/10.1038/s41598-019-51378-4>
77. Kelso B, Smith RV, Laughlin RJ, Lennox SD. 1997. Dissimilatory nitrate reduction in anaerobic sediments leading to river nitrite accumulation. *Appl Environ Microbiol* 63:4679–4685. <https://doi.org/10.1128/aem.63.12.4679-4685.1997>
78. Kofoed MVW, Stief P, Hauzmayer S, Schramm A, Herrmann M. 2012. Higher nitrate-reducer diversity in macrophyte-colonized compared to unvegetated freshwater sediment. *Syst Appl Microbiol* 35:465–472. <https://doi.org/10.1016/j.syapm.2012.08.005>
79. Hou L, Wang R, Yin G, Liu M, Zheng Y. 2018. Nitrogen fixation in the intertidal sediments of the Yangtze Estuary: occurrence and environmental implications. *J Geophys Res Biogeosci* 123:936–944. <https://doi.org/10.1002/2018JG004418>